Temperature and pH Dependence of the Metarhodopsin I−Metarhodopsin II Equilibrium and the Binding of Metarhodopsin II to G Protein in Rod Disk Membranes†

John H. Parkes, Scott K. Gibson, and Paul A. Liebman*

Department of Biochemistry and Biophysics, University of Pennsylvania Medical Center, Philadelphia, Pennsylvania 19104-6059

Received November 20, 1998; Revised Manuscript Received March 5, 1999

ABSTRACT: The equilibria between metarhodopsins I and II (MI and MII) and the binding of MII to retinal G protein (G) were investigated, using the dual wavelength absorbance response of rod disk membrane (RDM) suspensions to a series of small bleaches, together with a nonlinear least-squares fitting procedure that decouples the two reactions. This method has been subjected to a variety of theoretical and experimental tests that establish its validity. The two equilibrium constants, the amount of active G protein (that can bind to and stabilize MII) and the fraction bleached by the flash, have been determined without a priori assumptions about these values, at temperatures between 0 and 15 °C and pHs from 6.2 to 8.2. Binding of G to MII in normal RDM exhibits 1:1 stoichiometry (*not* cooperative), relatively weak, $2-4 \times 10^4$ M^{-1} affinity on the membrane, with a pH dependence maximal at pH 7.6, and a low thermal coefficient. The reported amount of active G remained constant even when its binding constant was reduced more than 10-fold at low pH. The method can readily be applied to the binding of MII to other proteins or polypeptides that stabilize its conformation as MII. It appears capable of determining many of the essential physical constants of G protein coupled receptor interaction with immediate signaling partners and the effect of perturbation of environmental parameters on these constants.

Members of the G protein coupled receptor (GPCR)[1] family number in the thousands, functioning to transduce extracellular signals that cells depend on for most of their life processes. GPCRs are postulated to exist in several intramolecular conformations. It is thought that signals (agonists) activate them by stabilizing the particular receptor conformation that binds to and activates G proteins. Receptor-bound G proteins lose their GDP and stabilize the receptor in the agonist-activated conformation. This paradigm appears to be qualitatively supported by data from many receptor systems that show the midpoint of agonist binding curves to be shifted to lower agonist concentration in the presence of G protein (the agonist-receptor high-affinity state) [see Kenakin (*1*) and references therein]. When GTP binding subsequently releases the bound G protein, the receptor returns to its low agonist affinity state.

The kinetics and thermodynamics of receptor−G protein interactions have resisted quantitative analysis partly because these proteins are restricted to the surfaces of cellular membranes where they are less accessible to common biochemical techniques. Difficulty in obtaining natural or recombinant receptor and G proteins in amounts necessary for many experimental approaches has also slowed progress.

Receptor−G protein interactions in rod disk membranes closely mirror those of other GPCRs. In its least active state, rhodopsin contains the inverse agonist and chromophore, 11-*cis*-retinal, which is covalently attached to the receptor protein. Light absorbed by rhodopsin can isomerize this chromophore to *all-trans*-retinal, the agonist of rhodopsin activation. Resultant protein charge redistribution and conformational changes produce rapid changes in rhodopsin's visible light absorption spectra, ultimately forming a pH and temperature-dependent equilibrium between metarhodopsins I (MI, λ_{max} 480 nm) and II (MII, λ_{max} 387 nm) (*2*, *3*). These spectroscopic properties of rhodopsin's activation path intermediates, together with the natural abundance of rhodopsin and retinal G protein, make possible the quantitative investigation of GPCR signaling events that have been virtually impossible to study in other GPCR systems.

MII is the first rhodopsin-bleaching intermediate able to bind the rod G protein, transducin (*4*), forming MII·G, the visual homologue of the agonist-receptor high-affinity state. Binding to G stabilizes MII (*5*), removing it from the MI-MII equilibrium and, in the absence of guanine nucleotides,

† Supported by NIH Grants EY00012, EY01583, and EY07035.

* To whom correspondence should be addressed. Phone: 215-898-6917. Fax: 215-573-8093. E-mail: liebmanp@mail.med.upenn.edu.

[1] Abbreviations: f, fraction of rhodopsin bleached per flash; G, G protein; GDP, guanosine 5′-diphosphate; GPCR, G protein coupled receptor; GTP, guanosine 5′-triphosphate; GTPγS, guanosine 5′-*O*-(3-thio-triphosphate); K_a, MI-MII equilibrium constant; K_b, MII·G binding constant; MI, metarhodopsin I; MII, metarhodopsin II; MIII, metarhodopsin III; MOPS, 3-(*N*-morpholino)propanesulfonic acid; OD, optical density; ΔOD, optical density difference; R, rhodopsin, R*, bleached rhodopsin; RDM, rod disk membranes; $[R]_{mem}$, $[R]_{sol}$, rhodopsin membrane phase or solution average concentration; sRDM, hypotonically stripped RDM; SSR, sum of squared residuals; usRDM, urea stripped RDM.

10.1021/bi9827666 CCC: $18.00
Published on Web 05/04/1999

producing an enhanced absorbance at 390 nm (*6*). Since MII·G has the same absorbance as MII, only that portion of MII·G formed at the expense of MI contributes to the absorbance increase. The two reactions are thus coupled, the magnitude of the increase depending both on the amount of MII·G formed and on the MI-MII equilibrium.

Determination of equilibrium constants for coupled sets of reactions is a common problem in biochemistry. Evaluation of a bimolecular binding constant normally requires titration of one of the reactants into the other, measuring the amount of product formed and free reactant remaining for each titration point. Nevertheless, analysis can be particularly difficult when it is not possible to separate the reactions for individual study or when it is desirable to examine the coupled set in situ, where the classic titration of one reactant will affect the final amounts of all of the coupled products. Membrane-phase reactions, in particular, make this a cumbersome if not completely daunting task.

Rod disk membranes (RDM), however, contain rhodopsin and G protein in a ratio (10−20:1) substantially different from the expected stoichiometry of their reaction (1:1). By using a series of brief light flashes, the ambient G protein can be titrated with small pulses of bleached rhodopsin. The smaller amount of G protein will be bound (at reasonable binding affinity) well before the rhodopsin is exhausted. By activating R with small pulses of bleaching light, an entire titration of ambient G with bleached rhodopsin (R*) can be performed on a single sample. The optical density changes at 390 nm can then be fit to a quantitative chemical reaction model that decouples the two reactions. This permits the simultaneous determination of all the essential parameters: the initial concentrations of rhodopsin (R) and active G protein (G), the MI−MII (K_a) and MII + G − MII·G (K_b) equilibrium constants, and the fraction bleached (f) by each flash.

This method eliminates the need for any a priori assumptions such as the amount of G protein, the fraction of rhodopsin bleached per flash, or the MI−MII equilibrium constant, as have been previously used in estimating the MII·G binding constant (*7*). It has proven particularly valuable where many titrations are needed to explore the role of intensive variables such as pH, temperature, ionic strength, or phosphorylation stoichiometry that may simultaneously alter several features of the coupled equilibria. In this study, the method was used to determine the pH and temperature dependence of the four parameters, G, K_a, K_b, and f, between pH 6.2 and 8.2 and from 0 to 15 °C.

We describe the mathematical analysis that calculates the best-fitting values for these four parameters from the kinetic record of a single titration, and present several experimental and computational tests of its reliability.

Mathematical Analysis. The "enhanced" reaction of R* with G is,

$$R \xrightarrow{\text{light}} MI \underset{K_a}{\rightleftharpoons} MII \underset{K_b}{\overset{G_{\alpha\beta\gamma}\bullet GDP}{\rightleftharpoons}} MII{\bullet}G_{\alpha\beta\gamma} + GDP$$

the GDP being released as soon as G binds to MII. Added GTP (*8*) or one of its analogues [or GDP, in sufficiently high concentration (*9*)] releases MII from G, returning the 390 nm optical density to the lower value of the MI−MII equilibrium alone. Thus, in the presence of GTP, the "unenhanced" reaction is

$$R \xrightarrow{\text{light}} MI \underset{K_a}{\rightleftharpoons} MII \overset{G_{\alpha\beta\gamma}\bullet GDP + GTP}{\underset{K_b}{\rightleftharpoons}} MII + G_\alpha{\bullet}GTP + G_{\beta\gamma} + GDP$$

This effectively reduces to

$$R \xrightarrow{\text{light}} MI \underset{K_a}{\rightleftharpoons} MII$$

The solution for enhanced MII formation requires two conservation and two equilibrium equations:

$$[R^*] = [MI] + [MII] + [MII{\cdot}G]$$

$$[G]_{total} = [G]_{free} + [MII{\cdot}G]$$

$$K_a = [MII]/[MI]$$

$$K_b = [MII{\cdot}G]/([MII] \times [G]_{free})$$

Unenhanced MII formation requires just two equations:

$$[R^*] = [MI] + [MII]$$

$$K_a = [MII]/[MI]$$

The equations are readily solved for [MI], [MII], [MII·G], and $[G]_{free}$ (part I in the Appendix) as a function of the parameters $[G]_{total}$, K_a, K_b, and f, the fraction bleached. The predicted change in optical density is

$$\Delta OD = \Delta[R^*]\Delta\epsilon_{(Rh\rightarrow MI)} + (\Delta[MII] + \Delta[MII{\cdot}G])\Delta\epsilon_{(MI\rightarrow MII)}$$

where the differential extinction coefficients are for the indicated transitions at the wavelength pair used in the spectrophotometric measurements.

EXPERIMENTAL PROCEDURES

Fresh bovine eyes were obtained from a local slaughterhouse (MOPAC, Inc, Soudertown, PA) and the retinas dissected under infrared light using image converters. Rod disk membranes (RDM) were prepared by sucrose flotation (*10*) in isotonic buffer (20 mM MOPS, 100 mM KCl, 2 mM $MgCl_2$, 1 mM DTT, and 0.1 mM EDTA, pH 7, 0 °C). They were stored in the same medium on ice at a rhodopsin concentration of 150−200 μM. Hypotonically stripped rod disk membranes (sRDM) were prepared by washing RDM three times in hypotonic buffer (10 mM MOPS, 1 mM DTT, and 1 mM EDTA, pH 7.0, 0 °C) as described (*11*) to remove G protein and other peripheral proteins. The amount of remaining G protein was assayed using the serial bleach titration method of this paper, and additional washes were performed as necessary to reduce the residual G protein detected to less than 0.05 μM per 10 μM rhodopsin. Urea-stripped rod disk membranes (usRDM) were prepared from sRDM by suspending in hypotonic buffer containing 5 M urea, incubating on ice for 1 h, centrifuging, and washing once with hypotonic buffer. The sRDM and usRDM were stored in isotonic buffer as above.

$G_{\alpha\beta\gamma}$ was purified from bovine retinas by the method of Baehr et al. (*12*) and individual subunits, G_α and $G_{\beta\gamma}$, by the method of Kroll and Phillips et al. (*13*). Purity was checked using overloaded Coomassie stained SDS−PAGE gels. Concentrations were determined by UV spectroscopy using ϵ_{280} = 36 700 for G_α·GDP, 55 700 for $G_{\beta\gamma}$, and 92 400 for $G_{\alpha\beta\gamma}$·GDP, as summed from ($M^{-1}cm^{-1}$) tyrosine = 1300, tryptophan = 5500, GDP = 8800, and the relevant amino acid composition. Purified proteins were snap frozen in 100 μL aliquots and stored in liquid nitrogen. Aliquots were rapidly thawed just before use. Optical density was monitored kinetically at 390 nm, where MII absorbance is near its maximum. Reference beam OD at 417 nm, near the isosbestic (isochromic) wavelength for the MI−MII transition, was subtracted to minimize effects of light scattering.

For the experiments used to determine the pH and temperature dependence of the parameters, an aliquot of the stock suspension of RDM was diluted into pH-adjusted MOPS buffer to a final rhodopsin concentration of 10−12 μM. GTPγS (500 μM) was added in one-half of the experiments to prevent accumulation of MII·G. Samples were cooled to the desired temperature in the thermally jacketed cuvette holder of an SLM-Aminco DW2000 dual beam spectrophotometer. Absorption spectra were measured in split beam mode, with MOPS buffer in the reference cuvette. Bleaching kinetics were measured in a single cuvette in dual beam mode, with the wavelength alternating (chopped) between 390 nm (sample) and 417 nm (reference) every 2 ms. The bleaching flash entered the cuvette from the side, orthogonal to the measuring beams.

For the titration experiments with G protein, suspensions of RDM, sRDM, or usRDM were diluted into MOPS buffer at pH 7, 1 °C, to which varying amounts of G protein (either $G_{\alpha\beta\gamma}$ or $G_\alpha + G_{\beta\gamma}$) in MOPS buffer were added. Complementary amounts of MOPS buffer not containing G were added to maintain the same dilution factor, yielding a final concentration of about 10 μM rhodopsin.

Each sample was bleached 19 times at 50 s intervals, using flashes of constant intensity delivered from an EG&G (Electro-Optics, Salem, MA) xenon flash unit (FX-199 tube with a PS-302 power supply and a 7 μF external capacitor) operated at 500−1000 V. The flashes were filtered to block (>2 OD) wavelengths shorter than 414 nm or longer than 690 nm. Each flash bleached 3−6% of the remaining visual pigment, depending on the voltage of the flash unit. With the amount of G protein and the binding constant, K_b, in the range normally encountered, 19 3% bleaches were generally sufficient to accurately determine the parameters. The number of bleaches was increased to 39 when necessary to ensure near exhaustion of ligand, when either G protein was augmented or binding to MII was weak, e.g., at low pH.

The energy of each of 50 consecutive flashes was periodically measured with an IL-700 integrating radiometer (Radiometer, Inc., Evanston, IL) and found to be constant to within a 1.1% standard deviation from the mean. Bleaching by the measuring beam was determined to be 0.25% during each 50 s interval when the monochromator was set for a three nm band-pass at the differential wavelength pair used.

Rhodopsin concentration was determined for each sample from its initial absorption spectrum using ϵ_{500} = 40 000 M^{-1} cm^{-1} and the Dartnall correction for light scattering[2] (*14*). For kinetic measurements, the differential extinction coefficients used were −5500 M^{-1} cm^{-1} for the transition from rhodopsin to MI and 33 000 M^{-1} cm^{-1} for the transition from MI to MII at this wavelength pair. These were determined by analyzing bleaches at pH 9, 0 °C, where almost all of the bleached rhodopsin goes to MI, and G protein titration experiments, where virtually all of the rhodopsin bleached by the initial flash forms MII·G. Since the differential extinction coefficients were obtained from experiments in which the rhodopsin concentration had been determined by this method, the choice of extinction coefficient for rhodopsin is arbitrary, canceling out in the calculations.

A single RDM preparation was analyzed at five different pHs (approximately 6.3, 6.7, 7.1, 7.6, and 8.1) and at four temperatures (nominally 0, 5, 10, and 15 °C) with and without GTPγS (40 experiments). Each set of experiments was completed within the week that the eyes were harvested. The pH of each sample, measured at room temperature after each experiment, was corrected to the experimental temperature using the thermal dependence of the p*K* of MOPS, −0.012 pH units/°C (*15*). The entire set of experiments was performed three times, for a total of 60 enhanced and 60 unenhanced experiments.

RESULTS AND DISCUSSION

Method of Analysis of Kinetic Data. Figure 1 shows typical kinetic recordings for unenhanced (A) and enhanced (B) formation of MII, at five pHs and at a temperature near 0 °C. The optical density during unenhanced formation of MII steadily increases or decreases, depending on whether the pH of the sample is below or above the isochromic point, where the optical density increase due to MII formation is just enough to offset the decrease in optical density due to the formation of MI. These incremental changes in optical density diminish uniformly with successive bleaches in proportion to the remaining unbleached visual pigment. The records exhibiting enhanced MII formation (B) show an abnormally large initial increase in optical density, due to formation of MII·G. Note that at pHs above the isochromic point, the enhanced kinetic records are biphasic, initially increasing until the G is largely exhausted, and then decreasing in parallel with the unenhanced records.

Time-averaged values of the optical density were calculated from data preceding the first flash, and from that following each flash, starting from the time at which the reaction had essentially reached equilibrium. Nineteen consecutive differences in optical density (ΔODs) were calculated from these averaged values. These ΔODs were analyzed using the equations in part I of the Appendix by a Nelder−Mead nonlinear least-squares fitting routine (Simplex) (*16*) to determine the total amount of G, the fraction of rhodopsin bleached by each flash, and the two equilibrium constants, K_a and K_b. Rhodopsin concentration in solution ($[R]_{sol}$) was usually determined from the initial RDM or sRDM spectrum, while rhodopsin concentration on the membrane ($[R]_{mem}$) was assumed constant at 10 mM for unbleached RDM preparations (see Membrane Localization of Reactants, below).

[2] [Rhodopsin] = $(1.1OD_{500} - 0.77OD_{600} - 0.33OD_{400})$/40 000 M^{-1} cm^{-1}.

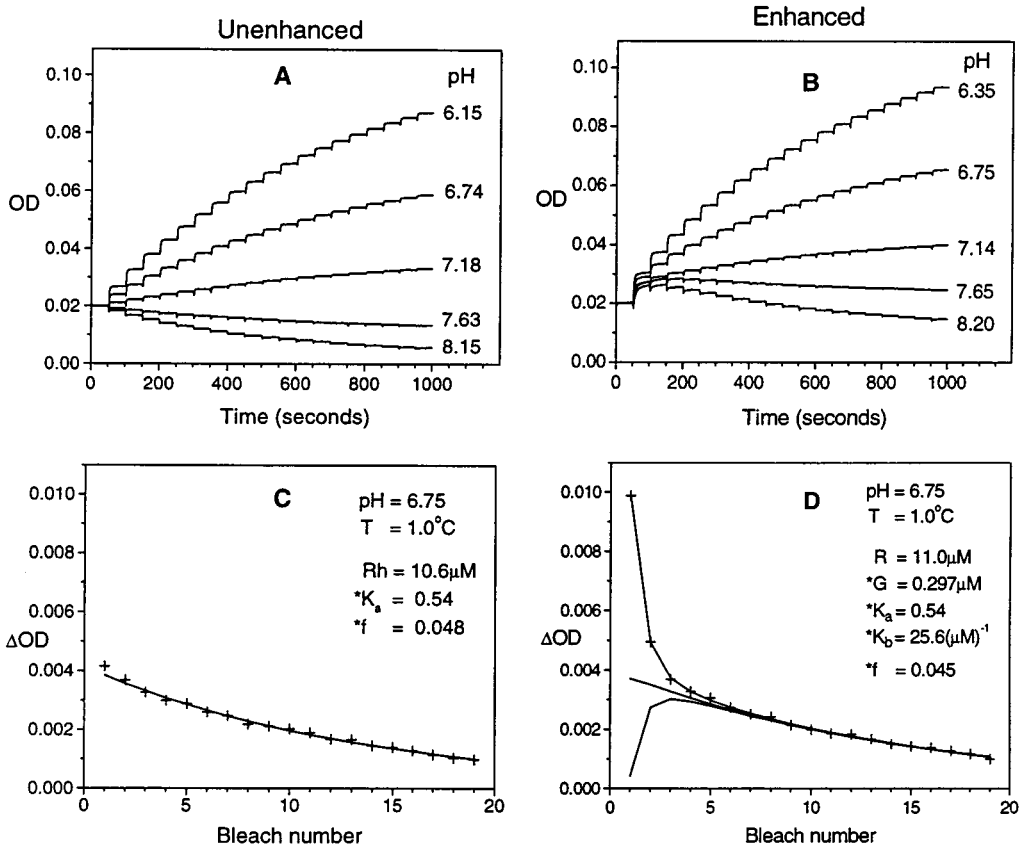

FIGURE 1: Optical density kinetics of five unenhanced (A) and five enhanced (B) preparations, recorded at 390/417 nm, in response to flash bleaches every 50 s. Temperature was 1 °C, pH as shown. Records showing enhancement have a large initial increase in OD at all pHs due to formation of MII·G. Equilibrium optical density differences between consecutive flashes (C and D) determined from lowest pH records in panels A and B. Symbols (+) are the changes in OD measured for each flash; the curve in panel C and the upper curve in panel D are the Simplex best-fit values for these ΔODs. The middle curve in panel D, calculated from K_a and f, is what the ΔODs would have been had there been no enhancement. The difference between the upper and lower curves in panel D shows the amount of MII·G formed by each flash. Parameters preceded by a star (*) were determined by Simplex analysis; R was fixed at the measured concentration.

Figure 1, panels C and D, plot the unenhanced and enhanced equilibrium data (ΔODs) obtained from the lowest pH kinetic traces shown in Figure 1, panels A and B. Simplex analysis curves that best fit these data and the values determined for the parameters are superimposed. With the pH and temperature closely matched, values for K_a and f for enhanced and unenhanced experiments are virtually identical, showing that the analysis successfully decouples the two reactions. The contributions to MII·G from MI and MII are in the ratio of 1 to K_a, since at equilibrium the fraction of bleached rhodopsin in MI is $1/(1 + K_a)$, while that in MII is $K_a/(1 + K_a)$, and the equilibrium is preserved when MII·G is formed.

Our Simplex program calculates the equilibrium concentrations of all of the rhodopsin intermediates and the free G after each bleach. Figure 2 shows how these concentrations evolve during the course of a 39-flash experiment for an RDM sample to which an additional 1.5 μM purified G had been added. Note that MII·G never attains a value equal to the starting concentration of G protein, nor does G_{free} go to zero, even after many bleaches, since the latter could at most bleach 10 μM rhodopsin, which would not bind all the G protein. [In fact, photoequilibrium would prevent even this much rhodopsin from being bleached (*17*).] This demonstrates that the amount of G determined by Simplex analysis includes both the free G and bound G (MII·G).

Membrane Localization of Reactants. While the rhodopsin concentration in solution varies with the experimental dilution factor, the rhodopsin concentration on an unbleached RDM is constant. Concentrations on a membrane or other surface should properly be expressed as moles per unit area. However, to make our values comparable to those reported

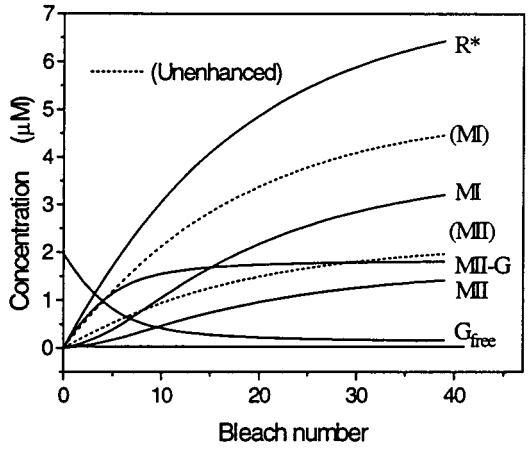

FIGURE 2: RDM (10 μM) preparation, containing ~0.45 μM G protein and augmented with an additional 1.5 μM G, bleached 39 times, and analyzed by the Simplex program. Graph shows evolution of rhodopsin intermediates and free G protein with successive bleaches. The Simplex program calculated total active G (MII·G + G_{free}) to be 1.961 μM. Note that MII·G never reaches this value, nor does G_{free} go to zero. Calculated values for unenhanced MI (upper) and MII (lower) dotted curves, based on the same values of K_a and f as for the enhanced data, are included for comparison.

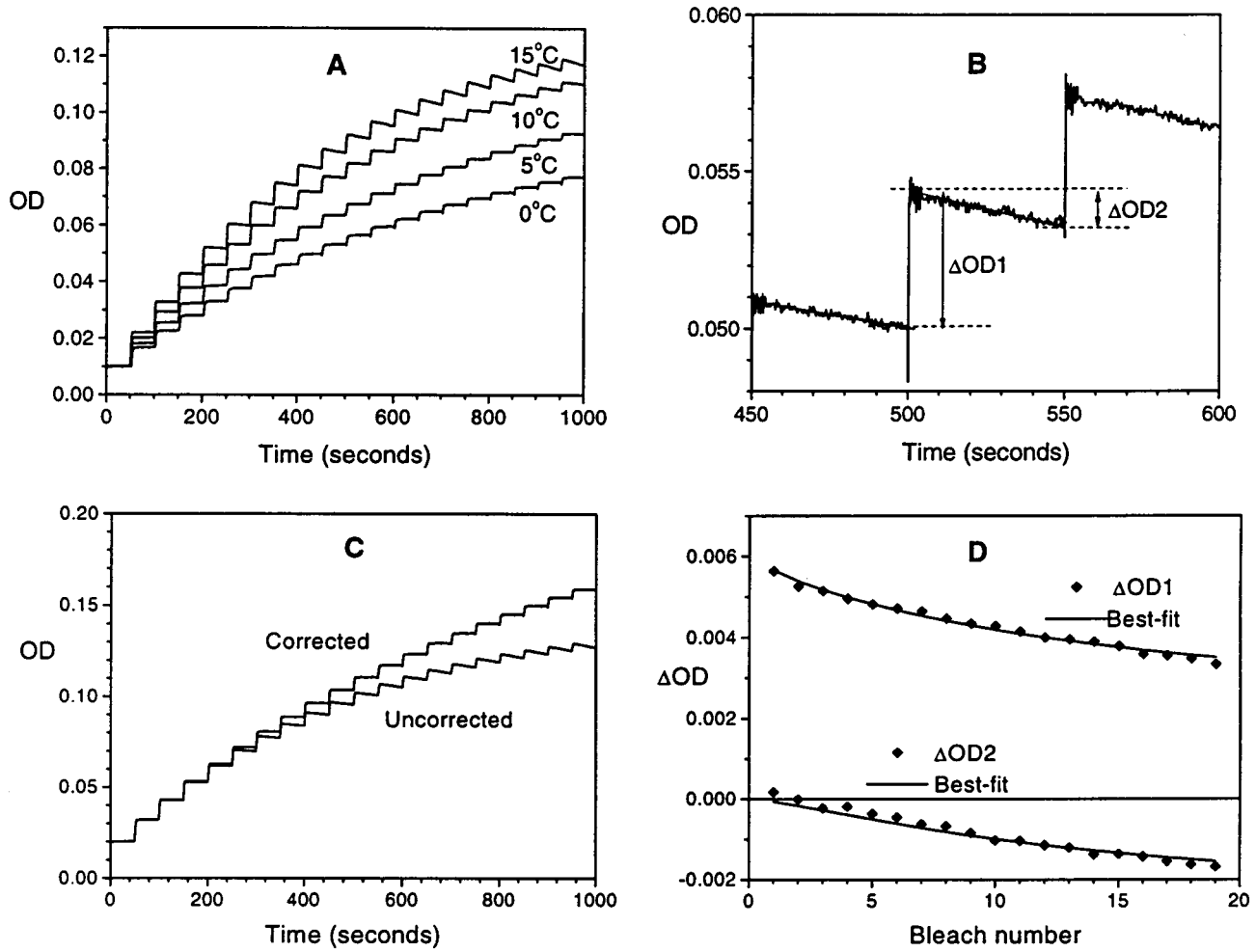

FIGURE 3: (A) Four unenhanced kinetic records of RDM preparations at pH 7 but at different temperatures, illustrating the increasingly rapid loss of OD between flashes with increasing temperature, due to conversion of MII to MIII. (B) Two ΔODs following each bleach were determined as shown. (C) Uncorrected (lower) and corrected kinetic records (upper trace), where smoothed values of the downward slopes of the lower trace (measured by ΔOD2) were added back, showing what the record would have been had there been no loss to MIII. (D) The two sets of ΔODs were analyzed simultaneously in terms of K_a, f, k_3 and k_{-3}, giving a measure of the amount of MIII formed.

in the literature, we express them as moles per unit volume, using the known thickness of the membrane. Since each rhodopsin molecule occupies an area of 36−40 nm^2 on the membrane (*18*), which has an effective thickness of about 4.5 nm, rhodopsin membrane concentration was calculated to be 10 mM. All of the reactions considered here (and GPCR-G protein interactions in general) occur on the membrane, so the reactants appear in the above equations at their membrane concentrations. The Simplex program uses the ratio of the solution-average rhodopsin concentration ($[R]_{sol}$) to that on the membrane ($[R]_{mem}$) after each iteration to calculate the solution-average concentration of all of the reactants and from them the optical density.

Equilibrium data from unenhanced preparations, to which GTPγS had been added, generally showed a small amount of enhancement with the first bleach. A possible explanation is that about 4% of the membranes isolated from a bovine rod are plasma membrane[3] which reseal with the G binding sites inside, effectively isolating a small fraction of the G from GTPγS (*19*). This enhancement was reduced to about 1% if the preparation was briefly sonicated with GTPγS, consistent with this fraction of vesicles having been inverted (data not shown). To minimize the effect of this slight MII enhancement on our analysis of unenhanced data, this first data point was excluded from the Simplex analysis of this class of experiments.

Correction for MIII Formation. At temperatures much above 1 °C, and especially at low pHs, the decay of MII was too rapid to be ignored. This produced a steady loss of optical density after the reaction forming MII·G should have reached equilibrium, as illustrated in Figure 3A. At the range of temperatures in our experiments, the free retinal formed should be negligible (*20*) so that the only decay product should be MIII. Although this may not be a homogeneous product (*21*), it was sufficient for our purposes to treat it like one, with an average differential extinction coefficient of about −10 000 M^{-1} cm^{-1}.

These kinetic records were analyzed using the two ΔODs illustrated in Figure 3B. ΔOD1 is the change in optical density between the end of one 50 s interval and the beginning of the next, and ΔOD2 is the change in optical density during the latter interval. Each is measured from the best-fit lines to the last 40 s of each interval. ΔOD1 is attributable to the change in concentration of rhodopsin, MI,

[3] A bovine rod 1.5 μm in diameter and 30 μm long has, at 33 disks/μm, a thousand disks with a total area of ∼3500 μm^2. The plasma membrane has an area of ∼140 μm^2, ∼4% of the total area.

MII, and MII·G due to bleaching and photoregeneration by the flash after they have reached thermal equilibrium. ΔOD2 is due to the same changes resulting from the bleach by the measure beam during the 50 s before the next flash, together with the formation of MIII during that time.

The rate of MIII formation should smoothly increase with the amount of MII formed during a series of bleaches, over the temperature and pH range studied. The 19 ΔOD2s were therefore smoothed by fitting to a single exponential. Where the best-fit value was negative (downward slope), an equivalent upward slope was added to the kinetic record, effectively eliminating any slope in the modified record (Figure 3C), which was then used in subsequent equilibrium analysis. This method maintains conservation of rhodopsin and its intermediates, showing what the data would have been if no MIII had formed, but it does not correctly treat photoregeneration from MIII. In effect, the method assumes that MIII has an efficiency of photoregeneration equal to an average of the efficiencies of photoregeneration of MI and MII (0.74 and 0.03 for our bleaching flash), weighted according to their relative concentrations, which will normally vary from one experiment to another.

A quasi-equilibrium method for estimating formation of MIII (Figure 3D) was developed to gain information about the kinetic parameters for the MII−MIII reaction, and to determine whether the standard equilibrium method produced significant error in the equilibrium constants. Since MIII formation never reached equilibrium under the conditions of these experiments, it had to be analyzed in terms of its first-order rate constants. In this method, the ΔOD1s were fit as before, but the ΔOD2s were simultaneously fit, using a kinetic analysis that tracked the rates of formation of MIII from MII (k_3) and regeneration of MII from MIII (k_{-3}), together with the known rate of bleaching by the measuring beam. We did not include MII·G with MII in calculating the forward rate with the Simplex program. Iterations were done every 5 s using a modified midpoint method, the amounts of MI, MII, MII·G, and MIII being corrected after each interval. After 50 s, the resulting change in OD was calculated, and compared with the measured ΔOD2 for that interval.

This gave us a measure of the amount of MIII formed in each experiment, permitting us to test limiting estimates for the relative quantum efficiency of photoregeneration from MIII, which was assigned the value of zero or that of MI. It provided reasonable estimates for the temperature and pH dependence of k_3 and k_{-3}, and confirmed that our standard method of analysis did not significantly affect the calculation of the equilibrium parameters.

Estimate of Errors. Probable errors of the best-fit values were obtained using a standard Monte Carlo method (Appendix III), since the Simplex program does not directly provide such estimates. K_a, the most precisely determined parameter, was found to be accurate to within 2% on individual experiments, f to 4−5%, total G to about 8−10%, and K_b to about 20%.

Validation of Simplifying Assumptions. Apart from the question of MIII formation, the Simplex analysis requires several simplifying assumptions that may be only approximately true. Once it was realized that the log decrement method[4] commonly used to calculate the fraction bleached generally gave erroneous values unless corrected for even very small amounts of photoregeneration (*17*), it became apparent that other approximations would also have to be checked to determine whether they produced similarly unexpected errors. For instance, successive flashes of equal intensity do not, in general, bleach exactly the same fraction of remaining visual pigment. If all of the bleached rhodopsin were immediately converted to colorless product, such as is the case for retinal oxime in the presence of hydroxylamine, then each succeeding flash would bleach a progressively larger fraction of the remaining rhodopsin, since, as the optical density decreases, there is less screening by other absorbers. This is also true when the bleaching product is MII or MII·G, since their absorption spectra overlap only slightly with that of rhodopsin.

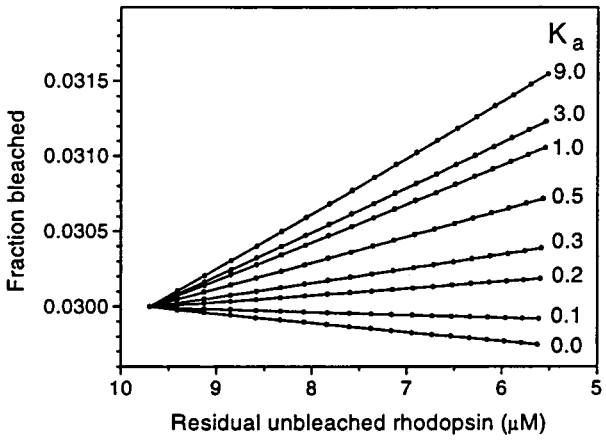

FIGURE 4: Effect of shielding by bleaching products on the fraction of rhodopsin bleached by successive flashes of constant intensity as a function of decreasing rhodopsin concentration. With sufficiently high K_a, the fraction bleached increases as the RDM suspension becomes progressively more transparent in the absorption region of rhodopsin. At low K_a, where most of the bleached rhodopsin is MI, the suspension becomes progressively more opaque, since MI is similar to rhodopsin in its absorption spectrum, and has a higher extinction coefficient.

When most of the bleaching product is MI, (e.g., at low temperature and high pH), the fraction bleached by successive flashes actually decreases, since the absorption spectrum of MI has its maximum close to that of rhodopsin and an extinction coefficient that is 25% larger. Thus, MI screens rhodopsin better than rhodopsin itself. This is illustrated in Figure 4, which shows the change in the fraction bleached as a function of K_a, corrected for screening but not for photoregeneration, which necessarily depends on the individual bleaching apparatus (*17*).

Another common assumption is that each flash bleaches the rhodopsin suspension uniformly across the width of the cuvette. Even in a semi-micro cuvette, however, there is significant attenuation of a bleaching flash across its four mm width. More than 30% of the 500 nm intensity passing through an RDM suspension containing 10 μM rhodopsin

[4] If the amount of rhodopsin bleached by each of a series of flashes of constant intensity is proportional to the remaining rhodopsin, then the size of the bleach will decrement by a constant ratio. If the logarithm of the bleach size is plotted vs bleach number, the plot will be linear, with the slope of ln(1 − f). Note, however, that the converse is not true; a log-linear slope does not necessarily imply that the bleach is proportional to the remaining rhodopsin.

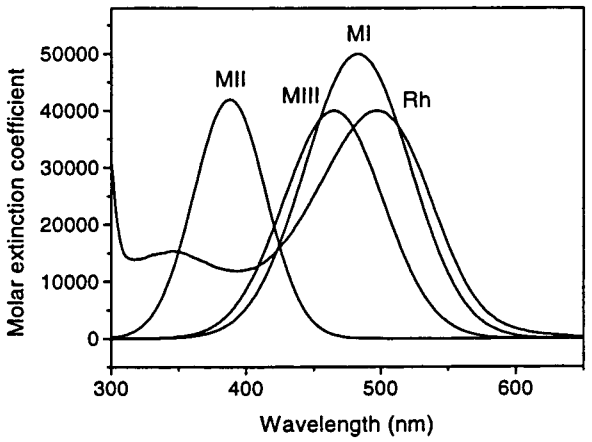

FIGURE 5: Absorption spectra of rhodopsin, metarhodopsin I, metarhodopsin II, and metarhodopsin III that were used to generate the artificial data employed to evaluate the accuracy of the Simplex analysis.

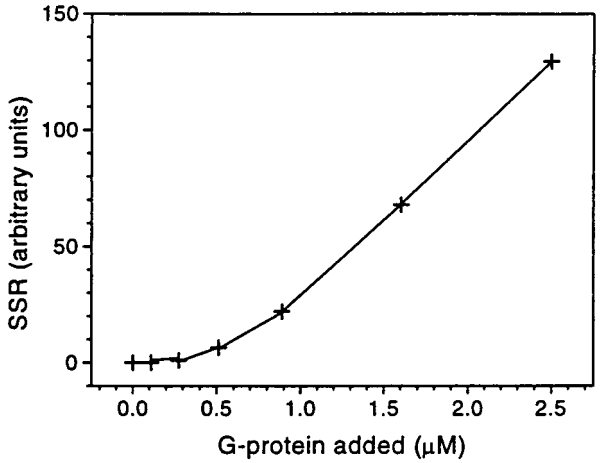

FIGURE 6: Increase in fitting error (SSR) from Simplex analysis of the G protein titration data when MII·G was assumed to photoregenerate like MII, compared to error when photoregeneration was assumed not to occur from MII·G. (This figure was presented at the annual meeting of the Association for Research in Vision and Ophthalmology in May 1994.)

is lost in this distance. Since the experimental absorbance is monitored orthogonally to the bleaching axis, the magnitude of the error produced by the inhomogeneity in optical density resulting from this flash attenuation profile might be appreciable. The error would be eliminated if there were complete intermixing of unequally bleached vesicles in the cuvette during the 50 s interval between flashes, but it is difficult to determine the extent of mixing. These uncertainties were resolved by computational modeling.

For this purpose, sets of artificial data were generated using specific values for the parameters. The data were then analyzed with the Simplex program to see if it reported the same values for the parameters that had been used to create the data. The modeled cuvette was 10 mm long by 4 mm wide, with a measuring beam passing through the long axis and a bleaching flash through the short axis, matching our experimental configuration. The modeling program utilized the output spectrum of the filtered bleaching flash, with the intensity measured at the position of the cuvette using an integrating radiometer and calibrated in absolute units of photons per flash. In the theoretical calculations, because of cumulative uncertainties in the absorption spectra of the intermediates and their quantum efficiencies of bleaching and photoregeneration, the measured intensity of a flash that bleached about 3% of a real visual pigment had to be adjusted to give an exact 3% bleach of a hypothetical sample. This obviated the need to make any correction for reflections of the bleaching flash by the optical faces of the cuvette.

The program calculated the overlap between the flash and the absorption spectra of rhodopsin, MI, and MII shown in Figure 5 and MII·G, which was assumed to have the same spectrum as MII. Absorption spectra for the metarhodopsins are not known exactly, but it was sufficient for this purpose to represent them by Gaussian curves with the correct molar extinction coefficients, wavelengths of maximum absorbance, and bandwidths. In analyzing the artificial data, we used the differential extinction coefficients taken from the curves. We assumed a temperature of 0 °C, so we did not have to consider formation of MIII. Spectral data were tracked at each of 259 wavelengths between 300 and 700 nm, the wavelengths at which our spectrophotometer reported its data.

The cuvette was then divided into 30 "slices", cut orthogonally to the direction of propagation of the bleaching flash, so that, with a total volume of 400 μL, each slice represented a volume 1 cm wide by 1 cm high by 0.013 33 cm thick. Using known quantum efficiencies for bleaching and photoregeneration,[5] we computed the light absorbed at each wavelength for each species of photopigment in each slice, the amount of bleaching or photoregeneration this produced and the amount of bleaching light at each wavelength that was transmitted to the next slice.

At the time these calculations were done, it was not known whether G protein binding would stabilize MII against photoregeneration. We therefore analyzed some of our G protein titration data assuming either that MII·G photoregenerated with the same quantum efficiency as MII or that it did not photoregenerate at all. If MII·G was assumed to photoregenerate, the fit to the data was consistently worse, and increasing amounts of MII·G resulted in increasingly poor fits (Figure 6). Our calculations therefore assumed no photoregeneration from MII·G. Subsequently, Arnis and Hofmann (*23*) reached the same conclusion, based on experiment evidence.

After completing these calculations, the thermal equilibrium values for MI and MII within each slice were computed. The program then either left the values of each species in each slice unchanged (unstirred) or replaced the concentration of each species with its average within the cuvette (stirred), so that the two limiting cases could be compared. The fractional optical transmissions of the two measuring beams at 390 and 417 nm were computed for each slice and then averaged, and from this, the optical density of the suspension that would be measured after each bleach was determined. From this, a data set was generated that could be analyzed by the Simplex. A major advantage of the artificial data was that the exact amount of rhodopsin bleached and photoregenerated by each flash was known, so that the true fraction bleached could be calculated. With real data, we could not

[5] Quantum efficiencies: bleaching of rhodopsin, 0.67; photoregeneration from MI and MII, 0.45 and 0.54. Taking into account the overlap between the filtered output of our bleaching flash and the action spectrum for each species, the efficiencies of photoregeneration from MI and MII, normalized to a value of 1.0 for rhodopsin bleaching, were 0.732 and 0.0298.

Table 1: Results of Simplex Analysis of Synthetic Data[a]

			values obtained from Simplex analysis			
			[R] fixed at 10 μM		[R] left as a free parameter	
	parameter	value used	stirred	unstirred	stirred	unstirred
unenhanced	R	10.0 μM	10.00*	10.00*	10.093	10.139
	K_a	0.5	0.5008	0.5005	0.4994	0.4989
	f	0.03	0.0299	0.0298	0.0299	0.0298
enhanced	R	10.0 μM	10.00*	10.00*	9.977	9.874
	G	0.6 μM	0.6007	0.6004	0.6019	0.6071
	K_a	0.5	0.5008	0.5020	0.5011	0.5036
	K_b	25.0 μM^{-1}	24.491	25.260	24.468	25.130
	f	0.03	0.0301	0.0299	0.0310	0.0302

[a] Synthetic, noise-free, 19-flash equilibrium data generated by a computer program using the values of the parameters on the left. Cuvette contents were modeled assuming either no interlayer diffusion ("unstirred") between bleaches, or complete diffusion ("stirred"), where the remaining [R], [MI], [MII], and [MII·G] were set to their average values after each bleach. The data were then analyzed by the Simplex program with initial [R] either fixed at 10 mM (*) or left as a free parameter. Values obtained from this analysis are shown in the four columns on the right.

Table 2: Comparison of Estimated Errors from Duplicates and from Monte Carlo Method[a]

method		G (μM)	K_a	K_b (μM^{-1})	f
direct measurement	mean	0.1745	0.4801	30.43	0.039 04
	sd	10.8%	1.95%	20.1%	5.6%
Monte Carlo simulation	mean	0.1746	0.4801	30.90	0.039 04
	sd	8.2%	1.4%	17.3%	4.2%

[a] Results obtained from duplicate experiments compared to those from Monte-Carlo simulation. Standard deviations (sd) are expressed as percentage of the mean.

directly check the accuracy of the reported fraction bleached, since the amount of bleached rhodopsin could only be calculated by using that value.

Table 1 compares the exact starting data with results obtained from the Simplex analysis of that data. The artificial data assumed a constant flash intensity, adjusted to give a 3% bleach of a previously unbleached 10 μM rhodopsin suspension. On subsequent flashes, the fraction bleached changed depending on the amount of rhodopsin remaining and the amount of shielding by the bleaching products. The calculations by the Simplex were greatly simplified, however, by assuming a constant bleach rather than a constant flash intensity. As can be seen, the reported results rarely differed from the exact values by more than 1−2%. Neither assumption (constant bleach or complete mixing) significantly affected the calculated values of the parameters.

The solution rhodopsin concentration directly determined from its absorption spectrum was normally used in the Simplex analysis of real experiments. If, however, the rhodopsin concentration was intentionally left as a free parameter, the Simplex analysis found its correct value, again to within 1−2% (Table 1), demonstrating the linear independence of the parameters.

Duplicates. Ten separate 19-flash experiments were performed using aliquots of the same prediluted RDM preparation. The 10 values for G, K_a, K_b, and f were averaged, and their standard deviations determined. The same sets of data were also analyzed using the Monte Carlo method, and the means and standard deviations of the ensemble determined. The results are compared in Table 2, with the standard deviation expressed as a percentage of the mean. The good agreement between the two methods confirms the adequacy of the assumptions made in using the Monte Carlo method, and the reasonableness of the estimated errors obtained from that analysis.

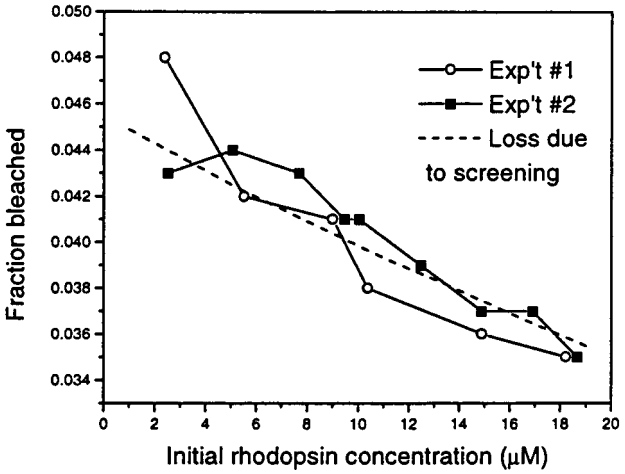

FIGURE 7: Decrease in the fraction bleached per flash as the initial rhodopsin concentration was increased, in two separate experimental series. Dashed line shows the predicted loss from pigment screening.

RDM Dilution. Aliquots of the same RDM preparation were analyzed over an 8-fold range of rhodopsin solution concentration; this was done with two different preparations. In the binding of MII to G, the relevant concentrations are those on the membrane. The membrane concentration of MII will not change with dilution, and the membrane-bound fraction of G protein, in equilibrium with a small aqueous fraction, will decrease only slightly. Thus, G, K_a, and K_b should be essentially constant, and the values found by the Simplex analysis proved this to be true (data not shown). The fraction bleached, however, would be expected to decline with increasing initial rhodopsin concentration due to greater screening. Figure 7 shows the fraction bleached vs rhodopsin concentration as determined for the two experiments and shows values for f calculated by the artificial data program at different rhodopsin concentrations. The increase in screening adequately explains the observed loss in fraction bleached.

Titration with G Protein. RDM, sRDM, or usRDM preparations were augmented with known, increasing amounts of G protein, and then assayed by the 39-flash Simplex analysis (Figure 8A). This experiment was carried out twice with RDM (12 titrations), three times with sRDM (20 titrations), and once with usRDM (five titrations) combined with $G_{\alpha\beta\gamma}$, or with G_α plus $G_{\beta\gamma}$. The results are shown in Figure 8B, where the total amount of G (MII·G + G_{free}) determined by the Simplex program is plotted against the

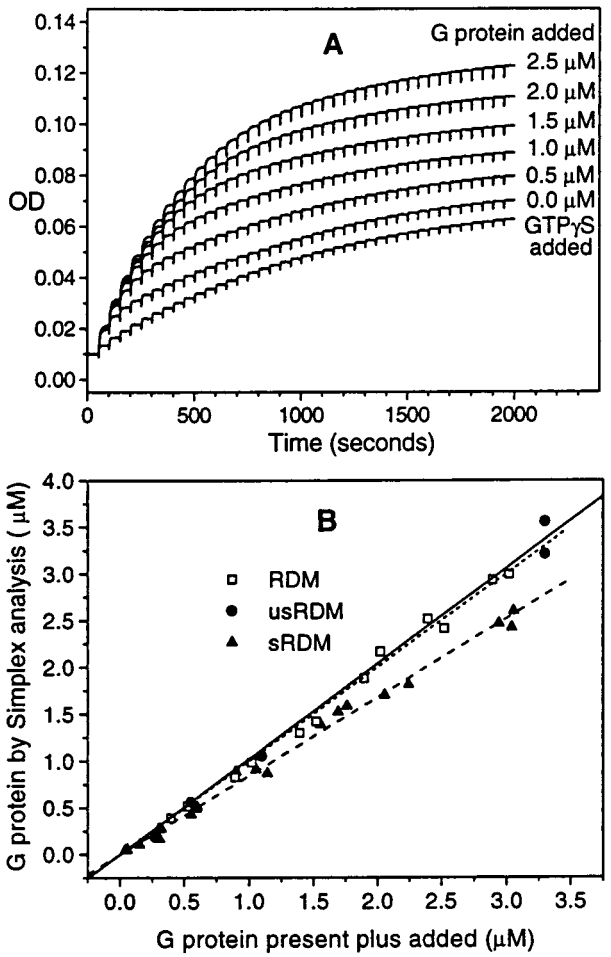

FIGURE 8: (A) Thirty-nine-flash records of RDMs titrated with increasing amounts of added G protein or with 100 μM GTPγS. G protein content measured by Simplex analysis is shown in Table 2. (B) Stoichiometry of binding of G to RDM, sRDM, and usRDM. Total G measured by Simplex analysis plotted against initial plus added G in six sets of titration experiments: two RDM, one usRDM, and three sRDM preparations. Slopes and standard deviations are RDM (long dash, 12 measurements), 1.00 $\pm$ 0.02; sRDM (short dash, 20 measurements), 0.84 $\pm$ 0.01; usRDM (solid line, five measurements), 1.02 $\pm$ 0.03.

sum of the amount of G protein already present plus that which was added. The total G protein was redetermined from the actual cuvette contents of each run by quantitative scanning of the Coomassie-stained SDS−PAGE gel bands of each preparation and compared to standards of known G protein concentration run on the same gel. The fractional yield of G protein in augmented preparations (measured G divided by G present plus added) was 1.00 $\pm$ 0.02 in RDM, 0.84 $\pm$ 0.03 in sRDM, and 1.02 $\pm$ 0.02 in usRDM. It made no apparent difference whether we used $G_{\alpha\beta\gamma}$ or $G_{\alpha} + G_{\beta\gamma}$ in the titrations.

Effects of Light Scattering. RDM and sRDM preparations scatter light significantly in the visible wavelengths, affecting both bleaching by the flash and measurement of optical density by the spectrophotometer. The path of an individual photon is altered by scattering, changing its path length in the cuvette and affecting the probability that it will be absorbed before it leaves the cuvette. Some photons travel a longer path before reaching the far side of the cuvette; others may be deflected out of the cell before traversing its full length. Whether the mean path length is shorter or longer than the length of the cell depends on its geometry; the wider the cell, the more likely it is that the scattered path will be greater than the cell's length. With a longer mean path length, the bleach will be greater for the same flash intensity.

With a cell that is 1 cm wide and 0.4 cm long, as seen by the flash, we found that normal RDM preparations bleach up to 10% more per flash than those that scatter less. This includes preparations that are older, have been hypotonically stripped of their peripheral proteins or sonicated to reduce the average vesicle size, and detergent extracts of rhodopsin (data not shown). In this case, the effect of scattering on the fraction bleached is real and will be accurately reflected in the Simplex analysis.

One consequence of this effect of scattering is that a flash cannot be calibrated using detergent-clarified rhodopsin to accurately determine the fraction bleached. The same flash bleaches significantly more pigment in an RDM preparation.

Scattering Wavelength Dependence. A 417 nm reference beam may not completely correct for the scattering at 390 nm. This causes a spurious change in the measured optical density increment, making it seem larger since scattering increases with decreasing wavelength. If the scattering is proportional to the amount of rhodopsin bleached or the amount of MI or MII formed, this can be taken into account in the differential extinction coefficients for the Rh-MI and MI-MII transitions, which include light lost through scattering as well as absorbance changes produced by these transitions.

If the differential light scattering is not proportional to the amount of rhodopsin bleached, but depends, for example, on the amount of MII·G formed (the so-called "binding signal"), the error will not be corrected by the extinction coefficients. Hofmann studied the binding signal extensively and concluded that use of the wavelength pair 380/417 nm almost totally eliminated these scattering contributions (*8*). Our more closely spaced reference and measure beams (390/417 nm) should provide an even better match.

Orthogonality of Parameters. The reliability of the method depends in large part on the near-orthogonality of the five parameters. The dependence of ΔOD in either enhanced (solid line) or unenhanced (dashed line) preparations on each of the parameters is shown graphically in Figure 9. In constructing these families of curves, a set of standard values was used: $[R]_{sol} = 10\ \mu M$, $[R]_{mem} = 10$ mM, $[G]_{mem} = 0.5$ mM, $K_a = 0.33$, $K_b = 100\ \mu M^{-1}$, and $f = 0.03$. In each graph, one of the parameters was varied; the others were assigned their standard values.

The shape of these parametric functions is perhaps best illustrated by subdividing each flash into small increments and rescaling the resulting ΔOD. A dramatic example is illustrated in Figure 9D, where, at very high K_b, an abrupt decrease in ΔOD occurs when the G protein is exhausted. The shape is also more easily appraised in semilogarithmic plots, where exponential decreases in ΔOD plot as straight lines.[6] The effect of varying f is more easily seen if $[R]_{mem}$ is varied inversely to hold the initial response constant.

[6] In the analysis of actual data, semilogarithmic plots have the disadvantage that they cannot be used to plot the biphasic response seen in enhanced preparations at pHs above the isochromic point. Experimental data are therefore all plotted linearly in this paper.

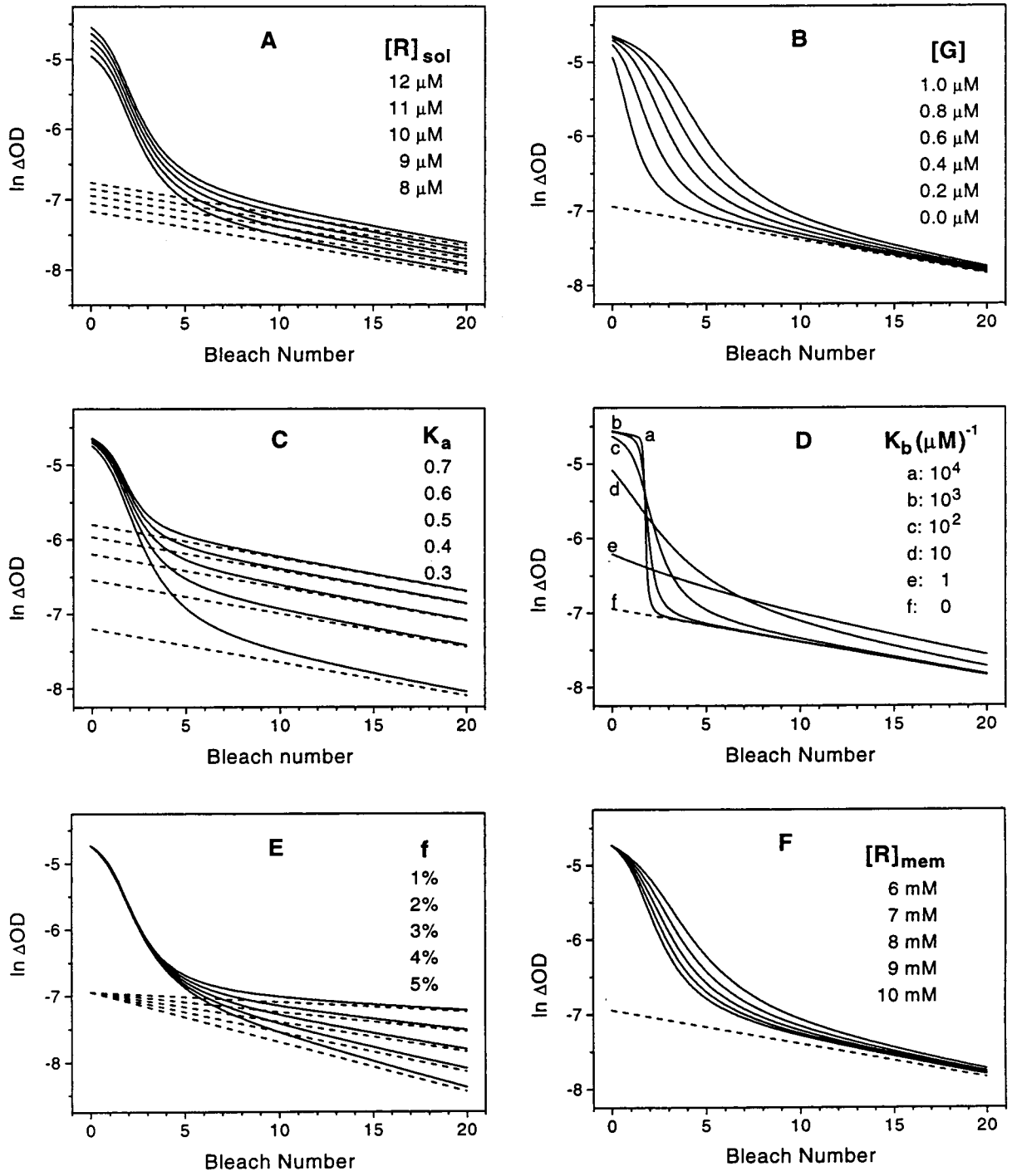

FIGURE 9: Enhancement curves synthesized to show characteristic shapes resulting from variation of a single parameter. Dashed lines show corresponding values for unenhanced data. Standard conditions were $[R]_{sol} = 10\ \mu M$, $[R]_{mem} = 10$ mM, $[G] = 0.5\ \mu M$, $K_a = 0.33$, $K_b = 100\ \mu M^{-1}$, and $f = 0.03$. In each figure, one parameter was varied as shown; the others had their standard values. The sets of curves (A−E) illustrate the point that these parameters are essentially orthogonal; each varies the curve in a unique manner. (F) This shows that changing the initial rhodopsin on the membrane is not the same as varying it in solution; the former affects the probability of interaction with G protein; the latter is simply a dilution of the membranes. Note that increasing $[R]_{mem}$ actually decreases the amount of enhancement. Since $[R]_{sol}$ is held constant, the number of RDMs in the sample decreases, and since $[G]_{mem}$ is held constant, $[G]_{total}$ decreases. Note also that $[R]_{mem}$ is not orthogonal to the other five; decreasing $[R]_{mem}$, while holding $[R]_{sol}$ constant, produces a change similar to increasing [G].

The five families of curves (Figure 9, panels A−E) illustrate the point that each parameter changes the shape of the enhanced response in a unique manner. Changing the rhodopsin concentration in solution (A) displaces the curve vertically, a quite different effect from changing the rhodopsin concentration on the membrane (F). Changing the G protein concentration (B) displaces and slightly stretches the curve horizontally. Changing K_a (C) stretches the curve vertically. Changing K_b (D) produces a major change in the maximum slope of the curve, which, for strong binding, occurs near the point where the total amount bleached equals the amount of G protein. Changing f (E), while maintaining a constant initial response, changes the slope of the asymptote of the final part of the curve. Since the parameters are essentially independent, reciprocal changes in two or more of the variables cannot compensate for one another.

Limitations of the Method. This independence of variables repeatedly proved itself in practice, provided there was enough bleached rhodopsin to bind most of the G protein. This assured that the last several ΔODs in a bleach series would decrease nearly exponentially. While the Simplex algorithm does not determine *f* from just the last few data points, if that portion of the data is almost log-linear, it imposes tighter constraints on the value of *f*. To the extent that determination of *f* is incorrect, the other parameters will also be in error. If K_b is weak ($<10\ \mu M^{-1}$) or *f* is small (<2%), it may be necessary to use a brighter flash or to increase the number of bleaches to meet this requirement.

Binding of MII to free G on the membrane is relatively fast, and even at 0 °C is completed well within the 50 s interflash interval. However, a small fraction of G (about one-sixth of total G in a 10 μM RDM suspension, for a K_D of 0.02 μM) is in the aqueous phase, in equilibrium with the free G on the membrane (*24*). This contributes to a slower component of MII·G formation, since, as the free G on the membrane is depleted by binding to MII, the membrane-partitioning equilibrium causes some aqueous phase G to shift onto the membrane, and this shift may not be complete within 50 s. When this happens, a small portion of the binding due to early flashes is displaced to later times. In this case, the program will still correctly calculate the total amount of G present, but will somewhat underestimate the value for K_b. The data acquisition protocol was therefore modified so that longer times could be allowed between the first few flashes. This allowed us to estimate the magnitude of the error in K_b when using constant interflash intervals, which proved to be not more then about 10%.

There are three other instances where the Simplex analysis may be less effective. (1) If the value of K_a is greater than 3, most of the bleached rhodopsin will already be MII, so that too little MI remains available to be converted to MII·G for much enhancement to occur. The value for K_b will thus become increasingly uncertain. (2) If the pH and temperature place the MI−MII equilibrium near its isochromic point, the small change in optical density makes the determination of *f* more uncertain. This results in corresponding uncertainties for the other parameters. In such cases, it may help to fix the value for one of the other parameters, if known independently. (3) If the fraction bleached is too large, so that all the enhancement occurs on the first flash, there is no upper limit to the value of K_b that will give a precise fit to the first data point, and the Simplex will report a very large, meaningless value. This can occur with too bright a flash or too little G protein. It is impossible to determine K_b from a single saturated data point; MII enhancement must extend over at least two bleaches to derive a meaningful value for K_b.

While the accuracy of the measurements is substantially improved when all four parameters are determined for each preparation, the cost of doing so is some degree of precision. Although the four parameters are essentially orthogonal in noise-free data, as was demonstrated above, this is no longer strictly true if the data is noisy, and as more variables are provided to the Simplex, the uncertainty in their best-fit values generally increases. Where it is possible to specify one or more of the parameters precisely, as was usually done with $[R]_{sol}$, the uncertainty in the other values is reduced.

Temperature and pH Dependence of Parameters. In these experiments, it was possible to examine the data from several points of view. The dependence of each parameter on pH, temperature, or particular set of experiments could be considered. Enhanced and unenhanced values could be compared or the correlation between parameters shown (e.g., Figure 7). Several points may be noted:

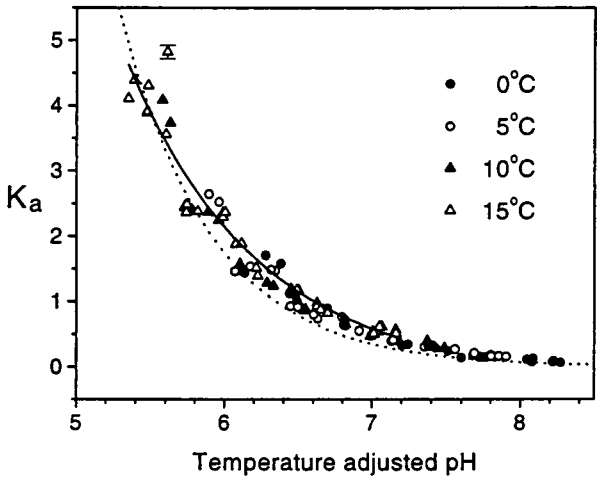

FIGURE 10: K_a as a function of temperature-adjusted pH. Error bars omitted if smaller than the symbol. If $\Delta pH = -\text{constant} \times \Delta T/(T + \Delta T)$, where ΔT is measured from 0 °C and ΔpH is the correction to the measured pH, the values for K_a lie on a smooth curve. Solid curve is the best fit to the present data. Dashed curve is the value for K_a calculated previously (*3*).

MI−MII Equilibrium Constant (K_a). The general formula for the pH and temperature dependence of K_a developed in the earlier paper on the MI−MII equilibrium (*3*), $\ln(K_a) = -9464/T - 1.608pH + 44.87$, where *T* is the absolute temperature, suggests that there is a tradeoff between temperature and pH. An increase in temperature has the same effect on K_a as a decrease in pH, where $\Delta pH = -\text{constant} \times \Delta T/[T(T + \Delta T)]$. Thus, the pH can be adjusted to compensate for differences in temperature, yielding a single smooth curve when K_a is plotted against the adjusted pH.

This is shown in Figure 10,[7] where the pHs were adjusted using a single constant to give a best fit of the K_as to a single exponential at 0 °C (solid curve). An increase in temperature from 0 to 5 °C is equivalent to a change of −0.344 pH units, an increase from 0 to 10 °C is equivalent to −0.675 pH units, and an increase from 0 to 15 °C is equivalent to −0.995 pH units. Also plotted on this figure is the value of K_a previously predicted (*25*) (dashed curve), which suggests that the numerical values from our previous work slightly underestimate K_a. Note that the methods used in the two papers are different; the earlier paper solved for K_a in terms of individual rate constants derived from kinetic measurements, while the present work depends solely on equilibrium values. More recent kinetic measurements give calculated values of K_a virtually identical to those reported here (*26*). The present data gives a p*K* for the MI−MII transition of 6.6 at 0 °C, somewhat higher than the earlier figure of 6.4.

Of the four parameters measured in this experiment, K_a is determined the most precisely, so that differences between preparations and even differences in the same preparation

[7] When used as a parameter, temperatures are the nominal ones; actual temperatures were held to within 1° of the nominal values. Error bars for individual data points were obtained by a Monte Carlo method (part III of Appendix). Where not shown, they are smaller than the size of the symbol.

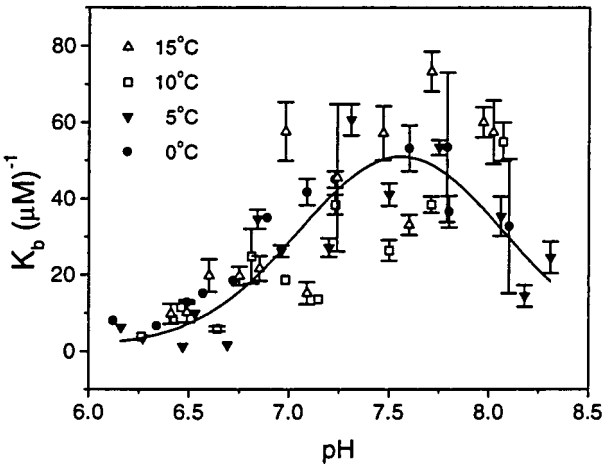

FIGURE 11: K_b plotted vs pH at four temperatures. Error bars omitted if smaller than the symbol. K_b appears to have a maximum at about pH 7.6 and approaches zero below pH 6.0. Curve is a best-fit double titration curve, with p*K*s at 7.15 and 8.0.

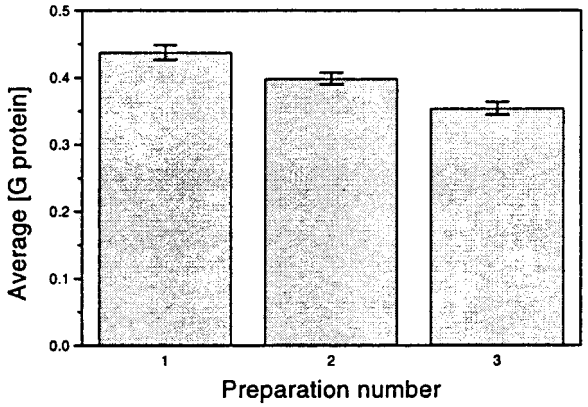

FIGURE 12: Variability of measured G protein concentrations within and among different RDM preparations. Standard errors of the mean (20 measurements) are shown at the top of each bar. The preparations were done by the same method in February, April, and June of the same year.

as it aged could be noted. In light of this sensitivity, the agreement between the values for K_a from the enhanced (solid) and unenhanced (open) data is significant. Had there not been good agreement between the enhanced and unenhanced values, we would have concluded that either the program was not able to deconvolve K_a and K_b, or that the two variables were not independent. Since there *is* good agreement, it can reasonably be concluded both that the Simplex analysis was well able to deconvolve the two coupled reactions and that K_a and K_b are indeed independent, as it is unlikely that any interdependence would just be offset by a failure to deconvolve the two over the entire range of temperature and pH studied.

MII·G Binding Constant (K_b). Figure 11 plots K_b vs pH at four temperatures. K_b has a pronounced pH dependence, maximal near pH 7.6, falling nearly to zero at pH 6, and apparently falling beyond pH 8. This decline at low and high pH could be explained by the presence of two protonatable sites on the relevant binding surfaces of either MII or G. When fit to a double titration curve, the two p*K*s are approximately 7.15 and 8.0. FTIR studies have shown a carboxylate of similar p*K* to be essential for G binding to MII to reside on rhodopsin (*22*). Binding thus would require the site with the higher p*K* to be protonated, but not the other. For values of K_a above three, the uncertainty in K_b greatly increases, for the reason discussed above.

Binding of MII to G appears to be somewhat tighter at higher temperatures (K_b larger), suggesting a hydrophobic component in the binding site. This slight temperature dependence of K_b contrasts with the pronounced temperature dependence of K_a. K_b was found to decrease significantly as preparations were increasingly augmented with G (about a 10-fold decrease in K_b if G is increased from 0.5 to 3 μM). This suggests steric or electrostatic hindrance to binding at high G concentration (data not shown).

G Protein. In contrast to the marked pH dependence of K_b, the computed values for G proved to be essentially constant with pH and temperature over the range studied. The pH dependence of G had a slope (millimolar active G protein on the membrane per pH unit) of 0.002 ± 0.005, while the temperature dependence had a slope (millimolar G per °C) of 0.0006 ± 0.0009; neither of which is significant. Thus, the Simplex analysis is consistently able to determine the same total amount of G protein, notwithstanding the large pH dependence in K_b. The drop in K_b by a factor of 10 or more apparently does not affect the ability of all the G to participate in binding to MII.

Where we did find a significant difference in the amount of G protein was among different preparations. Figure 12: set 1, in February, averaged 0.428 ± 0.017 mM (mean and standard error of the mean); set 2, in April, averaged 0.394 ± 0.010 mM; set 3, in June, averaged 0.346 ± 0.013 mM (each data set included 20 enhanced experiments). Whether these differences were due to small variations in the preparation conditions (the same method was used for all of them), to a seasonal variation, possibly due to the nutritional state of the cows, or to some other cause has not been determined. What is clear is that every preparation must be measured individually if these parameters matter; their values cannot be determined once and then used for all other RDM preparations.

Fraction Bleached. The value for *f* was nearly constant over the temperature and pH range studied. There was good agreement between enhanced and unenhanced data (not shown). As noted above, there was a significant increase of the uncertainty in *f* near the isochromic point for the MI−MII transition, which affects the other parameters.

Other Conformers of the Metarhodopsins. Recently, evidence has been developed that the traditional model of Rh → L → MI_{480} ⇔ MII_{380} is incomplete: that there is a MI_{380} transiently formed along with MI_{480} (*27*−*30*), that at least in certain detergents, there is an unprotonated form of MII_{380} that does not bind G protein (*23*, *31*), or that there are two protonated forms of MII_{380} (*32*). How would the present analysis be affected by these new intermediates?

The MI_{380} intermediate has not been observed below 20 °C, and when it is seen, it disappears within 100 ms at all pHs, so it should have no effect on our equilibrium measurements. Other isoforms of MII do not appear to be present at equilibrium in large amounts, and even if they themselves do not bind G protein, they are in equilibrium with isoforms that do. Our analysis shows that, with small bleaches and added G protein, the fraction of MII in the form of MII·G exceeds 95%. Thus, even if a nonbinding isoform of MII were present in RDM in substantial amounts in

Table 3: Simplex Analysis for One-Site and Two-Site Binding of G Protein to MII[a]

	R (μM)	G (μM)	K_a	K_{b1} (μM^{-1})	K_{b2} (μM^{-1})	f	SSR
one-site	10.0	0.293	0.547	11.84		0.0558	5.00×10^{-9}
two-site	10.0	0.326	0.548	10.60	1.321	0.0544	3.56×10^{-9}

[a] Results obtained by fitting averaged data (60 experiments) to one-site and two-site binding models of G protein to rhodopsin, with $[R]_{sol}$ fixed at 10 μM. Common parameters are similar in value, but K_{b2} is much smaller than K_{b1}, not 40 times larger, as was reported for urea stripped RDM (*28*).

equilibrium with protonated MII, the equilibrium would be shifted toward the binding isoform by the presence of G protein. K_a and K_b might then have to be interpreted somewhat differently, perhaps as the product of two equilibrium constants. However, the state of knowledge concerning these additional intermediates is too much in flux at the present time, with too little agreement among investigators, to justify further speculation.

Cooperative Binding. Several investigators studied the interaction of rhodopsin with G protein in bleached urea-stripped membranes and concluded that the binding is cooperative, with two G protein molecules binding to each bleached rhodopsin (*33*, *34*). Both groups used a large excess of bleached rhodopsin and varied the G protein concentration. The former studied the effect of rhodopsin vs no rhodopsin on the initial rate of GTPγS binding to G protein, while the latter measured the light−dark difference in the amount of G protein bound to RDM. Neither could measure the binding stoichiometry directly; both inferred it from the sigmoidal shape of the binding curves and the slope of associated Hill plots.

From our analysis, it is concluded that a 2:1 stoichiometry cannot be supported for normal RDM. The method described here determines the total concentration of G protein that is in equilibrium with MII and uses this, the amount of bleached rhodopsin, and the binding constant, K_b, to determine the number of MII·Gs that are formed. On the reasonable assumption that the extinction coefficient of MII·G does not differ significantly from that of MII, the MII·G formed very nearly equals (100 ± 2%) the G protein added. This is in agreement with much earlier work by Kuhn et al. (*35*), who inferred a 1:1 stoichiometry between photoexcited rhodopsin and G protein on hypotonically stripped RDM.

Test of Two-Site Model. The alternative stoichiometries for G binding to MII were examined quantitatively after solving the coupled equilibrium and conservation equations for two-site cooperative binding (part IV in the Appendix) and determining how the binding of a fixed amount of G protein would titrate with increasing amounts of bleached rhodopsin. Sixty enhanced 19-flash equilibrium records were averaged and then analyzed by a least-squares fitting routine for one- and two-site models. The results are shown in Table 3 (K_{b2} is the association constant between G and MII·G, forming MII·G_2).

Note that while the values obtained for the other parameters are quite similar in the one and two-site models, K_{b2} is about eight times weaker than K_{b1}, rather than 40 times stronger, as was previously reported (*34*). The fitted ratio of MII·G_2 to MII·G, calculated by this analysis, declines from about 0.16 to 0.017 as the amount of bleached rhodopsin increases. The sum of squared residuals (SSR) improves only slightly, which would be expected when an extra parameter is added to fit data that is not perfectly noise free. Thus, the Simplex analysis has essentially thrown out the second binding constant, again strongly suggesting that there is no cooperative binding of G protein to rhodopsin in normal RDM.

In three titrations of hypotonically stripped RDMs (Figure 8B), only about 84% of the added G protein was reported by the Simplex analysis as MII·G or G_{free}. The reasons for this are not entirely clear. If the binding to MII (K_b) were simply weaker in sRDM, this should not affect the measured amount of G, which remains constant even if K_b is only a tenth of its maximum (see above). The result might suggest some degree of cooperativity. However, in preliminary studies with urea-stripped RDM, 102 ± 2% of the added G was reported as MII·G or G_{free}. Further studies of these questions are presently underway, but it seems unlikely that the binding of MII to G is cooperative in any form of RDM.

MII·G Binding Constant (K_b). There have been several previous estimates of the strength of binding of activated rhodopsin to G protein. Kuhn et al. (*35*) added known amounts of purified G protein to hypotonically stripped RDM, then bleached with a series of calibrated light flashes. The increase in OD at 380 nm was compared to the light scattering "binding signal" at 708 nm. The near stoichiometry of the two signals led these investigators to conclude that binding was so tight as to preclude a back reaction from MII·G.

From its value based on solution-average concentrations, the binding constant, K_b, appears to be quite high, on the order of 20 μM^{-1}. On the membrane, however, where all concentrations are 1000-fold higher, the true value of K_b is a relatively weak 20 mM^{-1}. Nonetheless, the reactants will bind almost completely because of their very high membrane concentrations, which substantially exceed K_b^{-1}, or 50 μM. It can be easily calculated that if $G = 0.5$ mM and $K_a = 1.0$, then 0.4 mM R* will be 99.9% bound to G, and even 0.5 mM R* will be 98.6% bound to G. This high-binding fraction is easily mistaken for the complete, irreversible binding inferred in earlier studies. Not only are higher binding constants unnecessary to ensure effective yield under these circumstances, but their higher Gibbs binding energy would have a higher cost for release of G than is needed at the lower membrane phase K_b in GTP activation from this MII·G complex. Faster dissociation kinetics is a further consequence of weak binding that may be useful in ensuring rapid reaction progress.

Emeis et al. (*5*) investigated formation of excess MII in RDM, or hypotonically stripped RDM augmented with G protein, in response to a series of calibrated bleaches. They also concluded that the binding was irreversible (although our analysis of their data suggested a binding constant of 60−80 μM^{-1}). Hofmann et al. (*36*) later reported a K_d (dissociation constant) of (1.0−1.2) × 10^{-7} M [equivalent to a K_b (association constant) of 8.3−10 μM^{-1}]. At the same time, Parkes et al. (*25*) reported a K_b of 10−100 μM^{-1}, based on the present method of analysis, although not fit by a least-squares procedure.

Bennett and Dupont (*7*) titrated RDM using flashes calibrated in detergent extracts of rhodopsin and assumed a G protein concentration of 0.5 μM per 10 μM rhodopsin.

Using a quadratic formula similar to that in part I of the Appendix, they obtained a dissociation constant of about 10 nM (equivalent to $K_b = 100\ \mu M^{-1}$). Schleicher et al. (*37*) used enhanced MII formation to study the binding of MII to arrestin. They also employed a quadratic formula to obtain the amount of active arrestin and the binding constant for MII to arrestin. However, they used a bleach calibrated with detergent extracts of rhodopsin, and assumed that the MI−MII equilibrium constant was unchanged by the addition of arrestin. They have not applied the same method to the binding of MII to G protein.

Other studies have reported that binding of GTPγS to G protein is pH dependent when activated by bleached rhodopsin (*38*−*40*). Each of the studies found activity approximated by a bell-shaped curve with a maximum near pH 7.5, although each reported the activity at pH 6 to be at least half of maximal activity. This gave a measure of the relative activity of the G protein, but did not identify the site measured or give the amount of active G or its binding constant to MII. These results are in general agreement with the data shown here, except that our values for K_b fall off more rapidly below pH 7, at all temperatures studied. K_b does appear to increase at higher temperatures, especially at lower pHs, but these are conditions under which the enhancement method becomes increasingly ineffective, since K_a is already high.

Even the best of these other methods has the drawback that the fraction bleached, the MI−MII equilibrium constant, and, in Bennett and Dupont (*7*), the G protein concentration were assumed a priori. All of our experience has been that G protein content may vary significantly from one preparation to another, and that the fraction bleached, because of changes in scattering and photoregeneration, cannot be accurately calibrated independently (*17*), especially not by using a detergent solution of rhodopsin as the standard.

CONCLUSION

The method of analysis described in this paper provides a simple, quick, and effective means to simultaneously determine all four parameters involved in the binding of activated rhodopsin to G protein. It requires only a double beam (or dual wavelength) spectrophotometer and a computer with appropriate software and can be completed in less than an hour. Using this method, we have determined the pH and temperature dependence of the two equilibrium constants, confirmed their mutual independence, evaluated the pK of the MI−MII transition and the one pK and the conjectural second pK of the binding of G to MII, and demonstrated that the binding of R* to G protein is not cooperative in RDM. We explain the illusion of very tight binding of R* to G, even though the on-membrane binding constant, K_b, is relatively weak.

ACKNOWLEDGMENT

We thank Robert Sharp and Nancy Thornton for expert technical assistance.

APPENDIX

(I) Solution of Coupled Binding Reactions (One Site). A general solution for the system of coupled reactions (*25*, *37*)

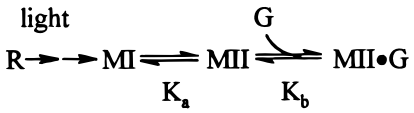

requires two equilibrium equations:

$$K_a = [MII]/[MI] \quad (A1)$$

$$K_b = [MII{\cdot}G]/([MII][G]_{free}) \quad (A2)$$

and two conservation equations:

$$[R^*] = [MI] + [MII] + [MII{\cdot}G] \quad (A3)$$

$$[G]_{total} = [G]_{free} + [MII{\cdot}G] \quad (A4)$$

To solve these for the four unknowns, [MI], [MII], [MII·G], and $[G]_{free}$, use eq A1 to eliminate [MI] from eq A3:

$$[R^*] = [MII]/K_a + [MII] + [MII{\cdot}G]$$
$$= [MII](K_a{+}1)/K_a + [MII{\cdot}G]$$

Then use eq A2 to eliminate [MII]:

$$[R^*] = ([MII{\cdot}G]/[G]_{free})(K_a{+}1)/(K_aK_b) + [MII{\cdot}G]$$

Finally, use eq A4 to eliminate $[G]_{free}$:

$$[R^*] = [MII{\cdot}G]/([G]_{total} - [MII{\cdot}G])(K_a{+}1)/(K_aK_b) + [MII{\cdot}G]$$

Transposing and collecting like powers of MII·G:

$$[MII{\cdot}G]^2 - \{[R^*] + [G]_{total} + (K_a + 1)/(K_aK_b)\}[MII{\cdot}G] + [R^*] \times [G]_{total} = 0$$

The roots of this quadratic equation are determined from the standard formula, $(-b \pm \sqrt{(b^2\text{-}4ac)})/2a$ (only the negative sign before the radical gives a physically meaningful solution), and the solution of the other three unknowns is then trivial. From these the optical density after each bleach can be calculated using the equation

$$OD = [R^*]\Delta\epsilon_{(Rh\rightarrow MI)} + ([MII] + [MII{\cdot}G])\Delta\epsilon_{(MI\rightarrow MII)}$$

where the two $\Delta\epsilon$s are the differential extinction coefficients for transitions from rhodopsin to MI ($-5500\ M^{-1}\ cm^{-1}$) and for MI to MII ($33\,000\ M^{-1}\ cm^{-1}$) at the wavelength pair (390 nm/417 nm) at which the data is measured. The formula assumes that, apart from photoregeneration, at equilibrium all of the bleached rhodopsin has been converted to MI and that some of it forms MII or MII·G.

For each flash, the program first determines the total amount of rhodopsin bleached, taking into account photoregeneration from the bleaching products. It then uses G_{total} and the equilibrium constants to recalculate the equilibrium values for MI, MII, MII·G, and G_{free}. From these, it calculates the optical density after each flash compares them with the data and readjusts the estimates for the free variables until it finds a best fit to the data.

(II) Effect of Photoregeneration on the Fraction Bleached. It was pointed out in an earlier paper (*17*) that correct

determination by the decrement method of the amount of visual pigment bleached by a series of small bleaches requires a knowledge of re, the relative efficiency of photoregeneration from those bleaching products present at the time of each flash. The amount bleached by the *n*th flash is the fraction bleached by a given flash times the amount of visual pigment remaining after the earlier bleaches, less the amount of product formed by those earlier bleaches times the fraction bleached times their relative efficiency of photoregeneration. That is,

$$b_n = R_{n-1}f - B_{n-1} \times \mathrm{re} \times f \qquad \text{(A5)}$$

where the three functions are defined as B_n, the fraction of rhodopsin or isorhodopsin bleached by n flashes, R_n, the fraction of rhodopsin or isorhodopsin remaining after n flashes, b_n, the fraction bleached by the nth flash. Defining the apparent bleach as

$$f_{\mathrm{app}} = 1 - (b_n/b_{n-1})$$

then the true bleach is

$$f = f_{\mathrm{app}}/(1 + \mathrm{re})$$

Although isorhodopsin has a lower quantum efficiency than rhodopsin for both bleaching and photoregeneration, we found that it could be treated like rhodopsin without producing a significant error in the calculations (*17*). Since

$$B_{n-1} = 1 - R_{n-1}$$

eq A5 can be written as

$$b_n = [R_{n-1}(\mathrm{re} + 1) - \mathrm{re}]\, f$$

This is the form used iteratively in the Simplex method to solve for the concentration of the intermediates.

Where the only bleaching products present at equilibrium are MI and MII, as is true in unenhanced RDM preparations, re is just the weighted sum of these two fractions:

$$\mathrm{re} = \mathrm{re1}\frac{[\mathrm{MI}]}{[\mathrm{MI}] + [\mathrm{MII}]} + \mathrm{re2}\frac{[\mathrm{MII}]}{[\mathrm{MI}] + [\mathrm{MII}]} = \frac{\mathrm{re1} + \mathrm{re2}K_a}{K_a + 1}$$

where K_a is the MI−MII equilibrium, and re1 and re2 are the relative efficiencies of photoregeneration from MI and MII, respectively. For a given value of K_a, re remains constant through the series of 19 bleaches.

With MII enhancement, three species are present at equilibrium: MI, MII, and MII·G. It was not known at the time that the experiments were analyzed whether binding to G protein stabilized MII against photoregeneration. The data were therefore fit to models with and without photoregeneration from MII·G. If there is photoregeneration from MII·G, then

$$\mathrm{re} = \mathrm{re1}\frac{[\mathrm{MI}]}{[\mathrm{MI}] + [\mathrm{MII}] + [\mathrm{MII{\cdot}G}]} + \mathrm{re2}\frac{[\mathrm{MII}] + [\mathrm{MII{\cdot}G}]}{[\mathrm{MI}] + [\mathrm{MII}] + [\mathrm{MII{\cdot}G}]}$$

Using the defining equations for the equilibrium constants, this can be expressed as

$$\mathrm{re} = \frac{\mathrm{re1} + \mathrm{re2}K_a(1 + K_b[\mathrm{G}]_{\mathrm{free}})}{1 + K_a(1 + K_b[\mathrm{G}]_{\mathrm{free}})}$$

If there is no photoregeneration from MII·G then

$$\mathrm{re} = \mathrm{re1}\frac{[\mathrm{MI}]}{[\mathrm{MI}] + [\mathrm{MII}] + [\mathrm{MII{\cdot}G}]} + \mathrm{re2}\frac{[\mathrm{MII}]}{[\mathrm{MI}] + [\mathrm{MII}] + [\mathrm{MII{\cdot}G}]}$$

which reduces to

$$\mathrm{re} = \frac{\mathrm{re1} + \mathrm{re2}K_a}{1 + K_a(1 + K_b[\mathrm{G}]_{\mathrm{free}})}$$

While K_a and K_b are constant throughout the series of bleaches, the value for G_{free} changes, declining toward zero as MII·G is formed. Thus, in analyzing an enhanced preparation, the value for re must be recalculated after each bleach. After a sufficient number of bleaches, where G_{free} is essentially zero, the equation for re reduces to the corresponding one for the unenhanced case, so that the enhanced and unenhanced curves are asymptotic.

Both photoregeneration and nonphotoregeneration equations were tried to see which gave the better fit to the data from the G protein titration, and the results were unambiguous (Figure 6). The fit was always worse if photoregeneration from MII·G was allowed, and it got increasingly worse as the amount of MII·G increased. We therefore assumed no photoregeneration from MII·G in our Simplex analysis. The same conclusion was subsequently reached by Arnis and Hofmann (*23*), based on their experimental data.

The value for re is known to be a function of pH and temperature through its dependence on K_a. Whether re1 and re2 themselves are temperature dependent remains unknown. The values for re1 and re2 for our apparatus were only determined for bleaches at zero degrees, because of the difficulty in measuring re at temperatures much above zero. We have assumed that re1 and re2 do not change significantly for temperatures up to 15 °C.

(III) Monte Carlo Method for Appraising the Reliability of Each Parameter. To estimate confidence limits associated with each parameter value, it was assumed that the standard deviations about the values actually obtained did not differ significantly from those about the true values (see, for example, Numerical Recipes in C, 1988) (*41*). Using the best-fit parameters obtained from the actual data, an exact set of equilibrium data was calculated. Normally distributed (Gaussian) deviations were generated using the *Box-Muller* method described in ref *41* and the random function generator provided by our computer. Individual deviations were then multiplied by an appropriate scale factor, so that the average error in the artificial data was similar to that of the real data.

This artificial data set was in turn analyzed by the Simplex and new values for the parameters determined. The process was repeated one thousand times for each set of real data, giving 1000 values for each parameter, from which standard deviations could be calculated. Finally, the standard deviations of the parameters in the artificial data were multiplied by the square root of the ratio of the sum of the squared residuals (SSR) of the real data to the SSR of the artificial

data, to make the average errors of the real and artificial data exactly equal.

A particular set of random errors would sometimes cause the Simplex to converge on a grossly improbable value for one or more of the parameters. This would distort both the average and standard deviation of the ensemble. The results from such a set of artificial data were therefore discarded if any one parameter differed from its corresponding value obtained from the real data by more that a factor of 10.

(IV) Solution of Cooperative Binding Equations (Two Site). Analysis of cooperative binding of two G proteins to one rhodopsin involves three equilibrium and two conservation equations:

$$K_a = [\mathrm{MII}]/[\mathrm{MI}]$$

$$K_{b1} = [\mathrm{MII{\cdot}G}]/[\mathrm{MII}][\mathrm{G}]$$

$$K_{b2} = [\mathrm{MII{\cdot}G_2}]/([\mathrm{MII{\cdot}G}][\mathrm{G}])$$

$$[\mathrm{R^*}] = [\mathrm{MI}] + [\mathrm{MII}] + [\mathrm{MII{\cdot}G}] + [\mathrm{MII{\cdot}G_2}]$$

$$[\mathrm{G}]_{total} = [\mathrm{G}] + [\mathrm{MII{\cdot}G}] + 2[\mathrm{MII{\cdot}G_2}]$$

where R* is the total amount of bleached rhodopsin and G is G_{free}. The first three equations can be written in terms of [MI]:

$$[\mathrm{MII}] = K_a[\mathrm{MI}]$$

$$[\mathrm{MII{\cdot}G}] = K_{b1}[\mathrm{G}][\mathrm{MII}] = [\mathrm{G}]K_aK_{b1}[\mathrm{MI}]$$

$$[\mathrm{MII{\cdot}G_2}] = K_{b2}[\mathrm{G}][\mathrm{MII{\cdot}G}] = [\mathrm{G}]^2K_aK_{b1}K_{b2}[\mathrm{MI}]$$

Then the last two equations can be written in terms of [MI] and [G]:

$$[\mathrm{R^*}] = [\mathrm{MI}](1 + K_a + [\mathrm{G}]K_aK_{b1} + [\mathrm{G}]^2K_aK_{b1}K_{b2}) \quad \text{(A6)}$$

$$[\mathrm{G}]_{total} = [\mathrm{G}] + [\mathrm{MI}]([\mathrm{G}]K_aK_{b1} + 2[\mathrm{G}]^2K_aK_{b1}K_{b2})$$

Solving both equations for [MI], equating them, and cross multiplying by the denominators:

$$([\mathrm{G}]_{total} - [\mathrm{G}])(1 + K_a + [\mathrm{G}]K_aK_{b1} + [\mathrm{G}]^2K_aK_{b1}K_{b2}) = \mathrm{R^*}([\mathrm{G}]K_aK_{b1} + 2[\mathrm{G}]^2K_aK_{b1}K_{b2})$$

Expanding these terms, and combining like powers of [G]:

$$[\mathrm{G}]^3(K_aK_{b1}K_{b2}) + [\mathrm{G}]^2\{K_aK_{b1} + (2[\mathrm{R^*}] - [\mathrm{G}]_{total})(K_aK_{b1}K_{b2})\} + [\mathrm{G}]\{K_a + 1 + ([\mathrm{R^*}] - [\mathrm{G}]_{total})(K_aK_{b1})\} - [\mathrm{G}]_{total}(K_a + 1) = 0$$

Dividing by $K_aK_{b1}K_{b2}$:

$$[\mathrm{G}]^3 + [\mathrm{G}]^2(2[\mathrm{R^*}] - [\mathrm{G}]_{total} + 1/K_{b2}) + [\mathrm{G}]\{(K_a + 1)/(K_aK_{b1}K_{b2}) + ([\mathrm{R^*}] - [\mathrm{G}]_{total})/K_{b2}\} - [\mathrm{G}]_{total}(K_a + 1)/(K_aK_{b1}K_{b2}) = 0$$

The cubic equation can be solved by standard methods (see, for example, ref *41*). If we abbreviate the coefficients of the cubic equation as:

$$a = 2[\mathrm{R^*}] - [\mathrm{G}]_{total} + 1/K_{b2}$$

$$b = (K_a + 1)/(K_aK_{b1}K_{b2}) + ([\mathrm{R^*}] - [\mathrm{G}]_{total})/K_{b2}$$

$$c = -[\mathrm{G}]_{total}(K_a + 1)/(K_aK_{b1}K_{b2})$$

and define

$$P = (a^2 - 3b)/9$$

$$Q = (2a^3 - 9ab + 27c)/54$$

then $D = P^3 - Q^2$ is the discriminant.

If $D >= 0$, there are three real roots, only one of which is positive. Set $X = \tan^{-1}\{\sqrt{(D)}/Q\}$, and get its principal value ($-\pi/2 < X \leq \pi/2$). The three roots are

$$\mathrm{root1} = -2\sqrt{(P)}\cos(X/3) - a/3$$

$$\mathrm{root2} = -2\sqrt{(P)}\cos[(X + 2\pi)/3] - a/3$$

$$\mathrm{root3} = -2\sqrt{(P)}\cos[(X + 4\pi)/3] - a/3$$

and G equals the one positive root.

If $D < 0$ there is only one real root. Let $E = [\sqrt{(-D)} + \mathrm{abs}(Q)]^{1/3}$. Then $G = -\mathrm{sign}(Q)(E + P/E) - a/3$.

From the value of [G], the bleaching intermediates and the OD can be determined, assuming that MII, MII·G, and MII·G_2 all have the same spectral absorbance. Solving eq A6 for MI,

$$[\mathrm{MI}] = [\mathrm{R^*}]/\{1 + K_a + ([\mathrm{G}]K_aK_{b1}) + ([\mathrm{G}]^2K_aK_{b1}K_{b2})\}$$

$$[\mathrm{MII}] = [\mathrm{MI}]K_a$$

$$[\mathrm{MII{\cdot}G}] = [\mathrm{MII}][\mathrm{G}]K_{b1}$$

$$[\mathrm{MII{\cdot}G_2}] = [\mathrm{MII{\cdot}G}][\mathrm{G}]K_{b2}$$

$$\mathrm{OD} = 0.033([\mathrm{MII}] + [\mathrm{MII{\cdot}G}] + [\mathrm{MII{\cdot}G_2}]) - 0.0055[\mathrm{MI}]$$

REFERENCES

1. Kenakin, T. (1996) *Pharmacol. Rev. 48*, 413−463.
2. Matthews, R. G., Hubbard, R., Brown, P. K., and Wald, G. (1963) *J. Gen. Physiol. 47*, 215−240.
3. Parkes, J. H., and Liebman, P. A. (1984) *Biochemistry 23*, 5054−5061.
4. Bennett, N., Michel-Villaz, M., and Kuhn, H. (1982) *Eur. J. Biochem. 127*, 97−103.
5. Emeis, D., Kuhn, H., Reichert, J., and Hofmann, K. P. (1982) *FEBS Lett. 143*, 29−34.
6. Emeis, D., and Hofmann, K. P. (1981) *FEBS Lett. 136*, 201−207.
7. Bennett, N., and Dupont, Y. (1985) *J. Biol. Chem. 260*, 4156−4168.
8. Hofmann, K. P. (1985) *Biochim. Biophys. Acta 810*, 278−281.
9. Panico, J., Parkes, J. H., and Liebman, P. A. (1990) *J. Biol. Chem. 265*, 18922−18927.
10. Yee, R., and Liebman, P. A. (1978) *J. Biol. Chem. 253*, 8902−8909.
11. Sitaramayya, A., and Liebman, P. A. (1983) *J. Biol. Chem. 258*, 1205−1209.
12. Baehr, W., Morita, E. A., Swanson, R. J., and Applebury, M. L. (1982) *J. Biol. Chem. 257*, 6452−6460.
13. Kroll, S., Phillips, W. J., and Cerione, R. A. (1989) *J. Biol. Chem. 264*, 4490−4497.

14. Knowles, A., and Dartnall, J. A. (1977) in *The Eye* (Davson H., Ed.) pp 53−101, Academic Press, New York.
15. Cooper, A., and Johnson, C. M. (1994) in *Microscopy, Optical Spectroscopy, and Macroscopic Techniques* (Jones, C., Mulloy, B., and Thomas, A. H., Eds.) pp 109−124, Humana Press.
16. Nelder, J. A., and Mead, R. (1965) *Comput. J. 7*, 308.
17. Parkes, J. H., and Liebman, P. A. (1994) *Biophys. J. 66*, 80−88.
18. Liebman, P. A., Parker, K. R., and Dratz, E. A. (1987) *Annu. Rev. Physiol. 49*, 765−791.
19. Adams, A. J., Tanaka, M., and Shichi, H. (1978) *Exp. Eye Res. 27*, 595−605.
20. Lewis, J. W., van Kuijk, F. J., Carruthers, J. A., and Kliger, D. S. (1997) *Vision Res. 37*, 1−8.
21. Hofmann, K. P., Pulvermuller, A., Buczylko, J., Van Hooser, P., and Palczewski, K. (1992) *J. Biol. Chem. 267*, 15701−15706.
22. Fahmy, K. (1998) *Biophys. J. 75*, 1306−1318.
23. Arnis, S., and Hofmann, K. P. (1995) *Biochemistry 34*, 9333−9340.
24. Schleicher, A., and Hofmann, K. P. (1987) *J. Membr. Biol. 95*, 271−281.
25. Parkes, J. H., and Liebman, P. A. (1984) *Invest. Ophthalmol. Visual Sci. (ARVO Supplement)* 156 (Abstr.).
26. Gibson, S. K., Parkes, J. H., and Liebman, P. A. (1998) *Biochemistry 37*, 11393−11398.
27. Thorgeirsson, T. E., Lewis, J. W., Wallace-Williams, S. E., and Kliger, D. S. (1992) *Photochem. Photobiol. 56*, 1135−1144.
28. Thorgeirsson, T. E., Lewis, J. W., Wallace-Williams, S. E., and Kliger, D. S. (1993) *Biochemistry 32*, 13861−13872.
29. Jager, S., Szundi, I., Lewis, J. W., Mah, T. L., and Kliger, D. S. (1998) *Biochemistry 37*, 6998−7005.
30. Szundi, I., Mah, T. L., Lewis, J. W., Jager, S., Ernst, O. P., Hofmann, K. P., and Kliger, D. S. (1998) *Biochemistry 37*, 14237−14244.
31. Arnis, S., and Hofmann, K. P. (1993) *Proc. Natl. Acad. Sci. U.S.A. 90*, 7849−7853.
32. Dickopf, S., Mielke, T., and Heyn, M. P. (1998) *Biochemistry 37*, 16888−16897.
33. Wessling-Resnick, M., and Johnson, G. L. (1987) *J. Biol. Chem. 262*, 12444−12447.
34. Willardson, B. M., Pou, B., Yoshida, T., and Bitensky, M. W. (1993) *J. Biol. Chem. 268*, 6371−6382.
35. Kuhn, H., Bennett, N., Michel-Villaz, M., and Chabre, M. (1981) *Proc. Natl. Acad. Sci. U.S.A. 78*, 6873−6877.
36. Hofmann, K. P., Reichert, J., and Emeis, D. (1984) *Invest. Ophthalmol. Visual Sci. (ARVO Supplement)* 156 (Abstr.).
37. Schleicher, A., Kuhn, H., and Hofmann, K. P. (1989) *Biochemistry 28*, 1770−1775.
38. Cohen, G. B., Oprian, D. D., and Robinson, P. R. (1992) *Biochemistry 31*, 12592−12601.
39. Fahmy, K., and Sakmar, T. P. (1992) *Biochemistry 31*, 12592−12601.
40. Surya, A., Foster, K. W., and Knox, B. E. (1995) *J. Biol. Chem. 270*, 5024−5031.
41. Press, W. H., Flannery, B. P., Teukolsky, S. A., and Vetterling, W. T. (1988) in *Numerical Recipes in C*, Cambridge University Press,

BI9827666